Plasmon-induced transparency in coupled triangle-rod arrays

To cite this article: Guang Yuan Si *et al* 2015 *Nanotechnology* **26** 025201

IOP Publishing Nanotechnology
Nanotechnology **26** (2014) 025201 (6pp) doi:10.1088/0957-4484/26/2/025201

Plasmon-induced transparency in coupled triangle-rod arrays

Guang Yuan Si[1,4], Eunice Sok Ping Leong[2,4], Wei Pan[3], Chan Choy Chum[2] and Yan Jun Liu[2]

[1] College of Information Science and Engineering, Northeastern University, Shenyang 110004, People's Republic of China
[2] Institute of Materials Research and Engineering, Agency for Science, Technology and Research (A*STAR), 3 Research Link, Singapore 117602, Singapore
[3] Pillar of Engineering Product Development, Singapore University of Technology and Design, 20 Dover Drive, Singapore 138682, Singapore

E-mail: liuy@imre.a-star.edu.sg

Received 14 October 2014
Accepted for publication 10 November 2014
Published 11 December 2014

Abstract

We demonstrate polarization-dependent plasmon-induced transparency in coupled triangle-rod arrays. The observed phenomenon is the result of the destructive interference between the bright and dark resonators in this coupled system, which is verified through the numerical simulations using the finite-difference time-domain (FDTD) method. By precisely controlling the structural parameters of the coupled triangle-rod system, the plasmon-induced transparency can be effectively manipulated. This plasmonically coupled nanostructure could be potentially useful for designing and developing artificial plasmonic molecules and metamaterials with desired functions, which may further find promising applications in biosensing, nanoparticle trapping and optical filters.

Keywords: plasmon-induced transparency, plasmon excitation, coupled metallic nanostructures

(Some figures may appear in colour only in the online journal)

1. Introduction

Electromagnetically induced transparency (EIT) is a quantum interference effect that eliminates light absorption in an atomic media [1, 2]. This phenomenon allows for a spectrally narrow optical transmission window accompanied with extreme dispersion, which is highly desirable for sensing and slow light applications [3, 4]. Recently, classical field interference that mimics the quantum EIT phenomena has been demonstrated as a means for the cancellation of absorption of electromagnetic waves propagating through artificially designed plasmonic nanostructures at a desired frequency, which would otherwise be nontransparent [5–11]. This phenomenon has been termed as plasmon-induced transparency (PIT) [5]. PIT involves strong coupling between two distinct plasmon resonance modes in a unit cell of the metallic nanostructures. One of the modes is highly radiative, providing a broadband resonance feature, and is called a superradiant 'bright' mode, while the other mode is a subradiant 'dark' resonator since it has a narrowband resonance. As a result, their destructive interference between strongly coupled bright and dark modes gives rise to a well-defined narrow transparency window. This narrow PIT window has great potential in many applications such as highly sensitive sensors [12–14] and rulers [15] and active PIT devices [16–19]. The artificially designed unit cell is of particular importance as the building block to construct plasmonic molecules and metamaterials with the desired optical functions. Small structural variations caused by the fabrication errors might cause significant deterioration of the optical functions.

Here, we will investigate the optical properties of coupled triangle-rod arrays. An apparent polarization-dependent PIT window is observed in their transmittance spectra. With precise tuning of the structural parameters, we further investigate the effect of the structural variation on the PIT window. Experimental results show that the PIT window can be

[4] These authors contributed equally to this work.

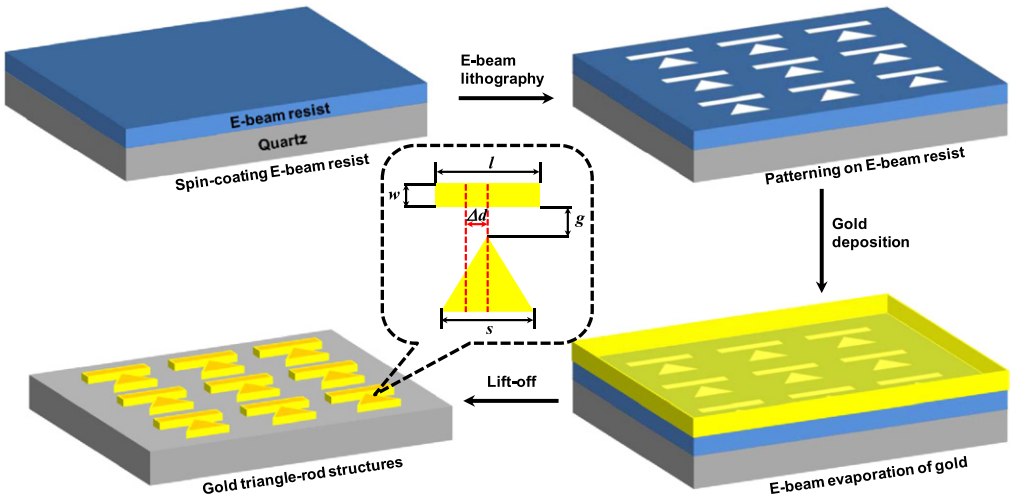

Figure 1. Typical fabrication process flow of the sample. The magnified inset shows a single unit with important structural parameters.

effectively manipulated. The fine-tuning of the structural parameters could also mimic the fabrication errors that should be considered in the design and performance evaluation of the PIT-based devices. Such plasmonically coupled nanostructures could be potentially useful for designing and developing artificial plasmonic molecules and metamaterials with certain functions and applications.

2. Experiment and simulation

2.1. Fabrication

The plasmonically coupled triangle-rod arrays were fabricated on a quartz substrate using electron-beam lithography (EBL), followed by metal evaporation and lift-off. Figure 1 shows the process flow (four steps in brief) of the sample fabrication. A 15 mm × 15 mm × 0.4 mm quartz substrate with a refractive index of 1.46 was cleaned with acetone and isopropyl alcohol (IPA) in an ultrasonic bath. A 10 nm thick indium-tin-oxide (ITO) layer was first sputtered onto the quartz surface using an unbalanced magnetron (UBM) sputtering system (Nanofilm). The purpose of the ITO layer is to provide a conductive surface on the quartz substrate for e-beam writing. To pattern the coupled triangle-rod arrays via EBL, a positive resist (PMMA 950 K) was spin-coated on the ITO/quartz to form a resist layer with a thickness of 250 nm (step 1). Pre-baking was carried out at 170 °C for 15 min. EBL was carried out with an ELIONIX ELS-7000 (step 2). The current and voltage used were 20 pA and 100 kV, respectively. Each pattern area was $50 \times 50\,\mu m^2$. The pattern development was done in MIBK:IPA (1:3) for 70 s. A short descum was carried out to remove any residual resist on the substrate using a reactive ion etching (RIE) Etcher (Plasmalab 80plus, Oxford) at 60 mTorr chamber pressure, 60 W electric power and a 60 sccm oxygen flow rate for 5 s. After that, two thin layers of titanium (3 nm) and gold (50 nm) were subsequently deposited using an e-beam evaporator (Denton Vacuum, Explorer) (step 3). The deposition of a titanium layer was used to enhance the adhesion of gold structures onto the quartz substrate. The deposition rate for each layer was controlled to 8 ± 2 nm min^{-1}. Finally, the coupled triangle-rod arrays were obtained after a lift-off process (step 4). The magnified inset in figure 1 shows a single unit of the coupled triangle-rod array, with the important structural parameters labelled. The side length of the equilateral nanotriangle (s) is set to 400 nm, and the length (l) and width (w) of the nanorod are 550 nm and 80 nm, respectively. The period of the coupled triangle-rod array is 2 μm. A series of triangle-rod arrays were fabricated with varying gaps (g) and an offset distance (Δd).

2.2. Characterization

The surface morphologies of the nanostructures were characterized using scanning electron microscopy (SEM). The transmission spectra were obtained using a UV–Vis–NIR microspectrophotometer (CRAIC QDI 2010 ™) with a 75 W broadband xenon light source. The probe light beam was focused to have a detecting area of $15 \times 15\,\mu m^2$ using a 36× objective lens combined with a variable aperture. The measured transmission was normalized with the light through a bare quartz substrate.

2.3. Simulation

To model the optical properties of the coupled triangle-rod arrays, we carried out the FDTD calculations using commercial software (Lumerical). The thickness of the structures was set to 50 nm, and the 3 nm thick Ti layer was ignored in the simulation. The dispersion of gold was based on the Johnson and Christy model in the material library of the software [20]. The triangle-rod structure was simulated with periodic (x- and y-directions) and perfectly matched layer (PML) (z-direction) boundary conditions. We impinged a plane wave with polarization either in the x- or y-direction from the bottom, reaching the quartz substrate first. A series of simulations were carried out with the two polarization directions for the different sets of gaps and displacements between the triangle and rod. The charge density was also

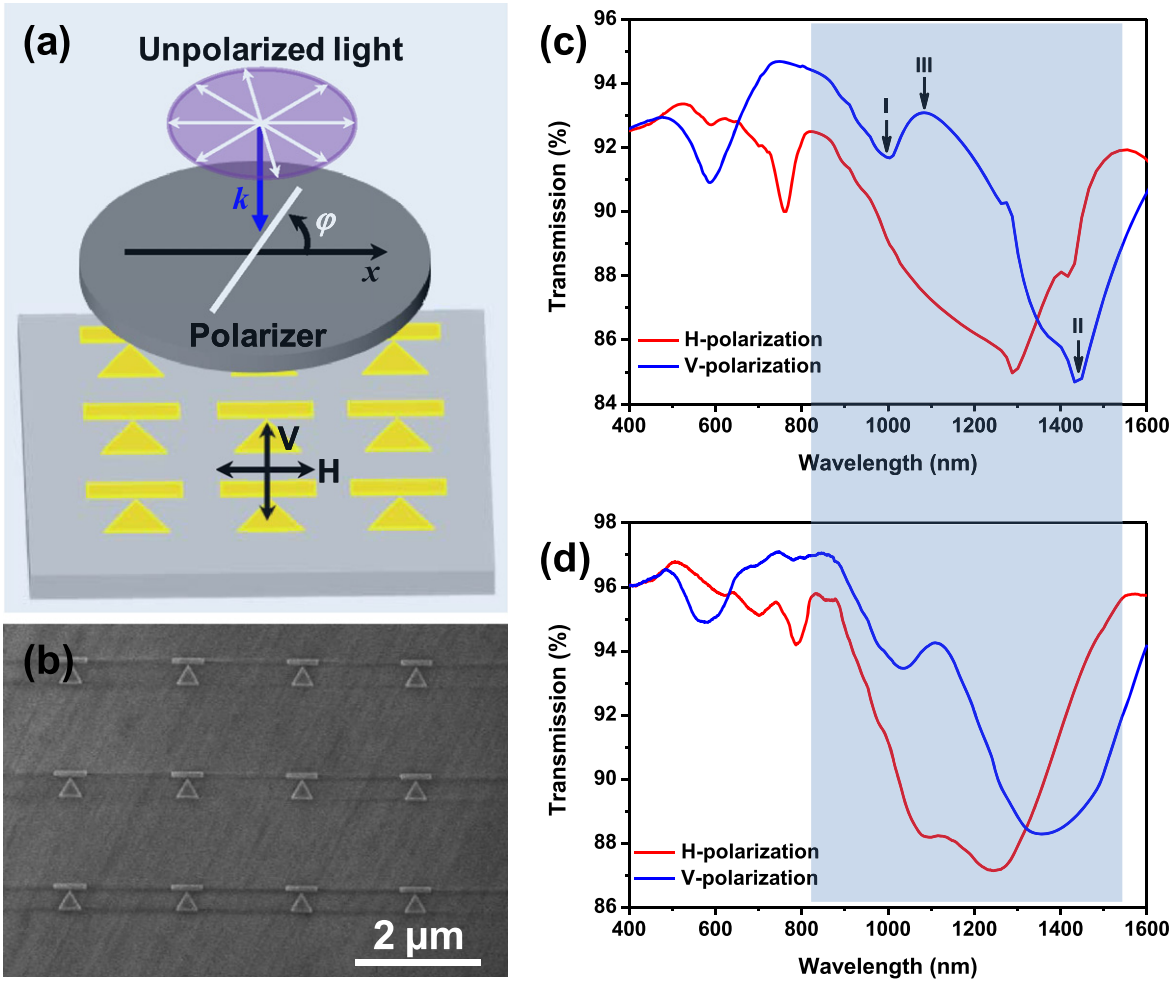

Figure 2. (a) Schematic of the experimental configuration. Horizontal (H) and vertical (V) polarizations of incident light are controlled by a linear polarizer. (b) SEM image of a representative coupled triangle-rod array fabricated by EBL. (c) Simulated transmission spectra under horizontally and vertically polarized incident light. (d) Experimentally measured transmission of the coupled triangle-rod array with $g = 20$ nm, $\Delta d = 0$ nm.

calculated to determine the distribution of charges in the structures.

3. Results and discussion

To have an overview of the PIT effect in our proposed structures, we took one fabricated sample and investigated it both numerically and experimentally. The experimental configuration is schematically shown in figure 2(a). A representative SEM image of the fabricated sample with the structural parameters ($g = 20$ nm, $\Delta d = 0$ nm) is shown in figure 2(b). The transmittance spectra are simulated under two different polarizations, as shown in figure 2(c). From the simulation results, we can see that for the H-polarization, there is only one broad dipolar dip, while for the V-polarization, an apparent peak (marked by III) rises from the broad valley when a nanorod is put in the vicinity of the nanotriangle. These observations can be further confirmed by the experimental results, as shown in figure 2(d). Overall, the spectral profiles of the simulations and experiments are in good agreement. Compared to the simulation results, the experimental PIT peak is slightly red-shifted, which could be mainly attributed to the shape tolerance and refractive index differences between the simulations and experiments.

To investigate the underlying nature of the appeared peak with the V-polarized light excitation, the electric-field and corresponding charge distributions at the labelled spectral positions are shown in figure 3. Figures 3(a)–(d) show the electric-field and charge distributions of dips I and II, which indicate that the nanotriangle and the nanorod are coupled as a dipole-multipole bonding (in-phase oscillation) mode at dip I and as a dipole-multipole antibonding (out-of-phase oscillation) mode at dip II. The triangle is resonant as a dipolar mode, while the nanorod has a multipolar mode with three parts of charges, which is in accordance with the eigenmode ($j = 2$) of a nanorod predicted by the electrostatic eigenmode method [21]. Figures 3(e) and (f) illustrate that peak III mainly originates from the multipolar mode ($j = 2$) of the nanorod. It is worth noting that the longitudinal nanorod plasmons cannot be directly excited to resonate under normally incident light with transverse polarization (i.e. the V-

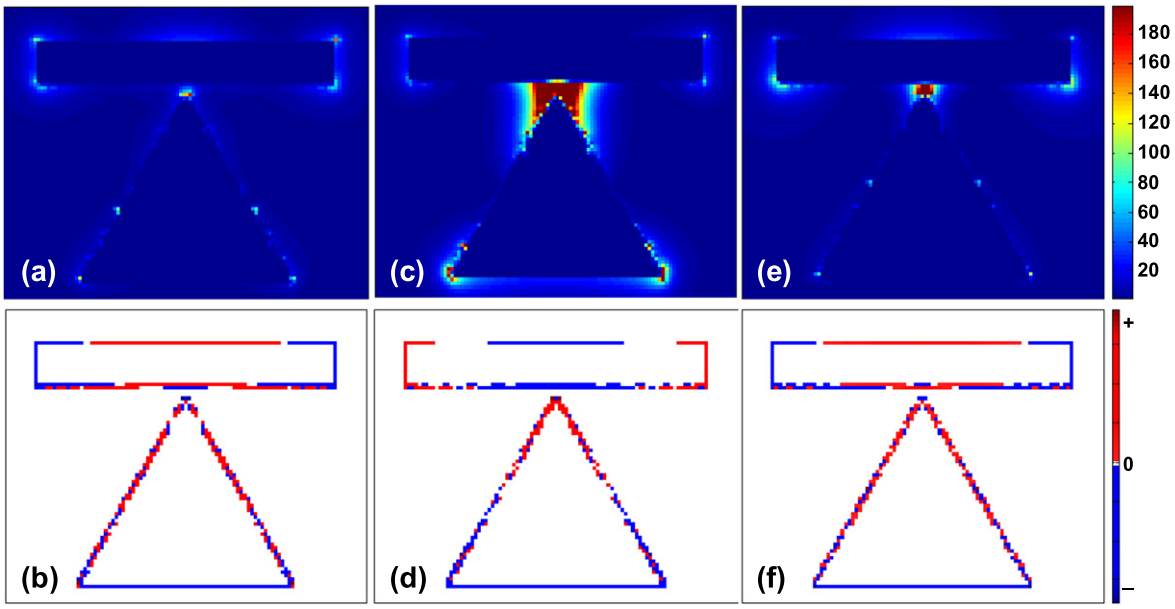

Figure 3. Electric-field (upper row: a, c and e) and charge (lower row: b, d and f) distributions at the labelled spectral positions I (a), (b), II (c), (d) and III (e), (f) in figure 2(c).

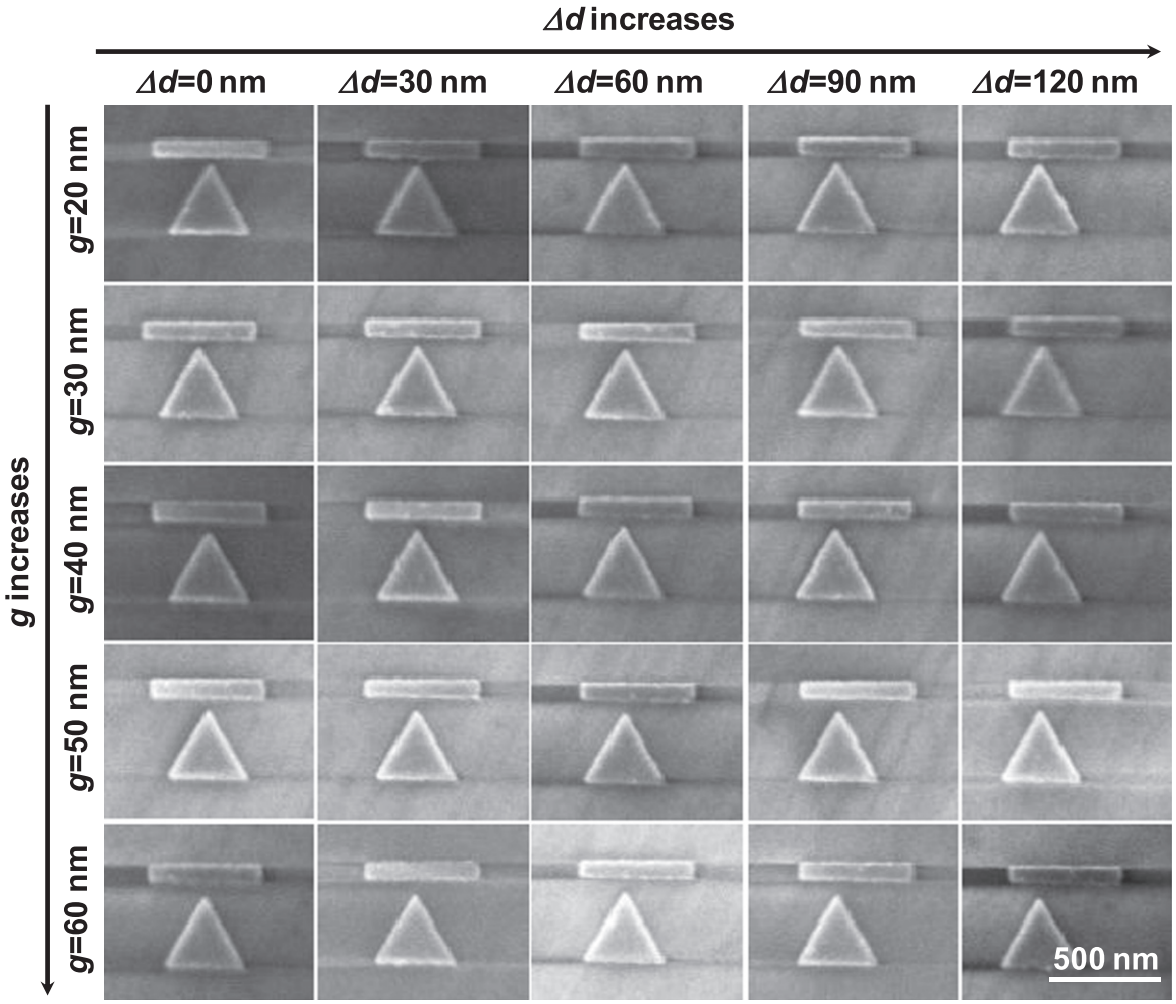

Figure 4. SEM images of the single unit cell of the coupled triangle-rod arrays with various gap sizes and offset distances.

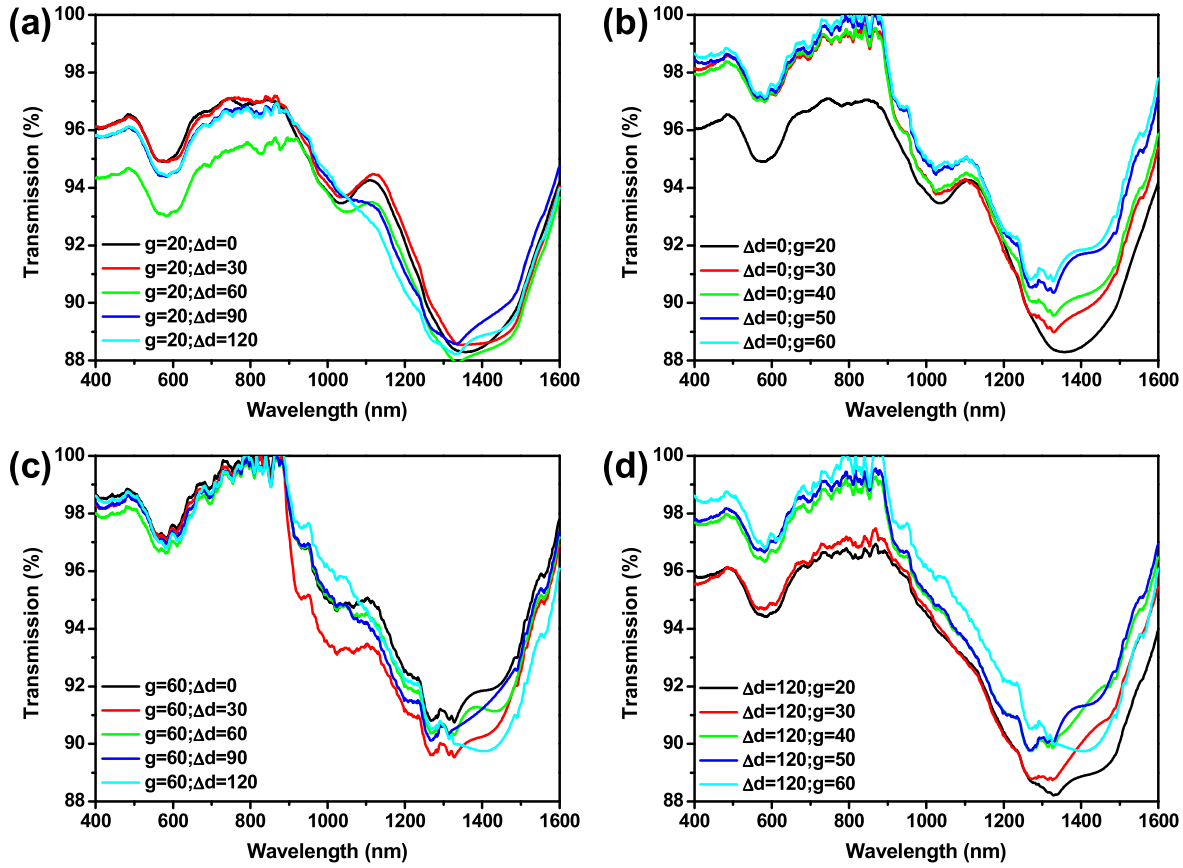

Figure 5. Measured transmission spectra of those circumjacent triangle-rod arrays in figure 4: (a) g = 20 nm, Δd = 0–120 nm; (b) Δd = 0 nm, g = 20–60 nm; (c) g = 60 nm, Δd = 0–120 nm; (d) Δd = 120 nm, g = 20–60 nm.

polarization in our definition). The electric-field distributions in figure 3 indicate that the multipolar mode ($j = 2$) of the nanorod is a result of the near-field excitation by the localized surface plasmon produced at the tip of the nanotriangle, which further facilitates the generation of the PIT phenomenon. In such a system, the nanorod serves as the dark resonator that is induced to be resonant as a multipolar mode ($j = 2$) with three charge nodes. From the above discussion, we conclude that such a coupled triangle-rod array demonstrates a polarization-dependent PIT window, which is mainly ascribed to the induced multipolar plasmon mode of the nanorod.

We further investigated the effect of small structural variations on the PIT window, which is usually met during the fabrication. Figure 4 shows typical SEM images of a single unit cell of the coupled triangle-rod arrays with various values of g and Δd. The gap between the nanorod and nanotriangle (g) is changed from 20 nm to 60 nm with the step size of 10 nm, whereas the offset distance Δd is increased from 0 to 120 nm in 30 nm increments. The transmission of each coupled triangle-rod array in figure 4 was then measured under the V-polarized light incidence. Figure 5 shows the experimental results of those representative arrays that are located in the circumjacent region. Although the measured transmission may vary slightly from one array to another, which is possibly caused by the defects or the characterization system inconsistency, a general trend can still be found from the extensive experimental results. At the fixed gap size of 20 nm, the PIT window gradually disappears with the increase of the offset distance (see figure 5(a)), while at the fixed offset distance, the transmission of the PIT window gradually increases with the increase of the gap size (see figure 5(b)). The PIT effect becomes very weak at both the large gap size (see figure 5(c)) and offset distance (see figure 5(d)). In our experiments, at the largest offset distance of 120 nm, the PIT effect totally disappears regardless of any gap size since the coupling strength between the nanotriangle and the nanorod becomes very weak, and the dark mode of the nanorod resonator cannot be excited. From the experimental results in figure 5, we can conclude that the coupling strength between the two modes can be effectively manipulated by precise tuning of the structural parameters. Comparatively, the offset distance has a much stronger effect on the PIT window than the gap size.

4. Conclusions

To summarize, we have demonstrated a polarization-dependent PIT window in coupled triangle-rod arrays. In this coupled triangle-rod system, the nanotriangle played as a bright resonator, which further excited the multipolar plasmon mode of the nanorod that served as a dark resonator. The observed PIT window was the result of the destructive

interference between the bright and dark resonance modes in this coupled system. With accurate tuning of the structural parameters, the PIT window can be effectively manipulated. The precise tuning of the structural parameters could also mimic the fabrication errors that should be considered for the design and performance evaluation of the PIT-based devices. This plasmonically coupled nanostructure could be potentially useful for designing and developing artificial plasmonic molecules and metamaterials with the desired functions, which may further find promising applications in biosensing, nanoparticle trapping and optical filters.

Acknowledgments

This work was financially supported by the Joint Council Office (JCO) of the Agency for Science Technology and Research (A*STAR) under grant No. 12302FG012.

References

[1] Boller K-J, Imamoglu A and Harris S E 1991 *Phys. Rev. Lett.* **66** 2593
[2] Harris S E 1997 *Phys. Today* **50** 36
[3] Lal S, Link S and Halas N J 2007 *Nat. Photon.* **1** 641
[4] Liu C, Dutton Z, Behroozi C H and Hau L V 2001 *Nature* **409** 490
[5] Zhang S, Genov D A, Wang Y, Liu M and Zhang X 2008 *Phys. Rev. Lett.* **101** 047401
[6] Liu N, Langguth L, Weiss T, Kastel J, Fleischhauer M, Pfau T and Giessen H 2009 *Nat. Mater.* **8** 758
[7] Artar A, Yanik A A and Altug H 2011 *Nano Lett.* **11** 1685
[8] Cetin A E, Artar A, Turkmen M, Yanik A A and Altug H 2011 *Opt. Express* **19** 22607
[9] Liu H, Li B, Zheng L, Xu C, Zhang G, Wu X and Xiang N 2013 *Opt. Lett.* **38** 977
[10] Biswas S, Duan J, Nepal D, Park K, Pachter R and Vaia R A 2013 *Nano Lett.* **13** 6287
[11] Chai Z, Hu X, Zhu Y, Sun S, Yang H and Gong Q 2014 *Adv. Opt. Mater.* **2** 320
[12] Chen C-Y, Un L-W, Tai N-H and Yen T-J 2009 *Opt. Express* **17** 15372
[13] Liu N, Weiss T, Mesch M, Langguth L, Eigenthaler U, Hirscher M, Sönnichsen C and Giessen H 2010 *Nano Lett.* **10** 1103
[14] Dong Z-G, Liu H, Cao J-X, Li T, Wang S-M, Zhu S-N and Zhang X 2010 *Appl. Phys. Lett.* **97** 114101
[15] Liu N, Hentschel M, Weiss T, Alivisatos A P and Giessen H 2011 *Science* **332** 1407
[16] Kurter C, Tassin P, Zhang L, Koschny T, Zhuravel A P, Ustinov A V, Anlage S M and Soukoulis C M 2011 *Phys. Rev. Lett.* **107** 043901
[17] Gu J *et al* 2012 *Nat. Commun.* **3** 1151
[18] Miyamaru F, Morita H, Nishiyama Y, Nishida T, Nakanishi T, Kitano M and Takeda M W 2014 *Sci. Rep.* **4** 4346
[19] Meng D, Wang S, Sun X, Gong R and Chen C 2014 *Appl. Phys. Lett.* **104** 261902
[20] Johnson P B and Christy R W 1972 *Phys. Rev.* B **6** 4370
[21] Davis T J, Gómez D E and Vernon K C 2010 *Nano Lett.* **10** 2618